International Journal of Pharmaceutics 413 (2011) 271–278

Contents lists available at ScienceDirect

International Journal of Pharmaceutics

journal homepage: www.elsevier.com/locate/ijpharm

Pharmaceutical Nanotechnology

Organic nanotubes for drug loading and cellular delivery

Ai Wakasugi[a], Masumi Asakawa[b], Masaki Kogiso[b], Toshimi Shimizu[b], Mamiko Sato[c], Yoshie Maitani[a,*]

[a] Institute of Medicinal Chemistry, Hoshi University, Tokyo, Japan
[b] Nanotube Research Center (NTRC), National Institute of Advanced Industrial Science and Technology (AIST), Tsukuba, Japan
[c] Laboratory of Electron Microscopy, Japan Women's University, Tokyo, Japan

ARTICLE INFO

Article history:
Received 11 March 2011
Accepted 15 April 2011
Available online 21 April 2011

Keywords:
Organic nanotube
Cellular uptake
Drug loading
Folate modification
Drug release
Doxorubicin

ABSTRACT

Organic nanotubes made of synthetic amphiphilic molecules are novel materials that form by self-assembly. In this study, organic nanotubes with a carboxyl group (ONTs) at the surface were used as a carrier for the anticancer drug doxorubicin, which has a weak amine group. The IC_{50} values of ONT for cells were higher than that of conventional liposomes, suggesting that ONTs are safe. The results showed that the drug loading of ONTs was susceptible to the effect of ionic strength and H^+ concentration in the medium, and drug release from ONTs was promoted at lower pH, which is favorable for the release of drugs in the endosome after cellular uptake. ONTs loaded with the drug were internalized, and the drug was released quickly in the cells, as demonstrated on transmission electron microscopy images of ONTs and the detection of a 0.05% dose of ONT chelating gadolinium in the cells. Moreover, ONT could be modified chemically with folate by simply mixing with a folate-conjugate lipid. Therefore, these novel, biodegradable organic nanotubes have the potential to be used as drug carriers for controlled and targeting drug delivery.

1. Introduction

Particle dosage forms have been receiving much attention as drug delivery systems (DDS), because of features such as controlled release, absorption improvement, and drug targeting. A variety of drug carriers, such as liposomes and polymer micelles, have been investigated (Bangham et al., 1965; Yokoyama et al., 1991), and their efficiency depending on carriers is reported. Currently, non-spherical carriers have received attention. Nonspereical particles were internalized in HeLa cells (Gratton et al., 2008). In this regard, we focused on organic nanotubes as a novel drug carrier. Organic nanotubes have a cylindrical structure that self-assembles from amphiphilic molecules in aqueous media. Organic nanotubes have an inner diameter of 10–200 nm, an outer diameter of 40–1000 nm, and a length of approximately 2 μm to several hundred μm. Furthermore, these dimensions are controllable by rationalizing the molecular structure of the amphiphilic molecules (John et al., 2001; Kamiya et al., 2005; Shimizu et al., 2005; Kogiso et al., 2007). Organic nanotubes can entrap proteins, nucleic acids, viruses, and metal nanoparticles, which cannot be achieved using cyclodextrin because organic nanotubes have at least a 10-fold larger inner diameter providing much greater space for the encapsulation of passenger molecules than cyclodextrin. Similar to cyclodextrin, organic nanotubes are expected to be applied for use in the medical and food fields (Yang et al., 2004a,b; Yui et al., 2005; Shimizu, 2006, 2008a; Kameta et al., 2005, 2007, 2008).

Organic nanotubes were first discovered to self-assemble from amphiphilic molecules in the pioneering work of Yager and Schoen (1983), Kunitake's (Nakashima et al., 1984), and Hirayama's (Yamada et al., 1984) research groups, among others, using diacetylenic phospholipids and glutamate derivatives. However, applications for these organic nanotubes have not been studied because the efficient mass production of these molecules has never been achieved. Interestingly, after the self-assembly of newly designed molecules in alcoholic solvents, such as ethanol, we found that evaporation of the solvent left tubular material in quantities more than 1000-fold greater than those when using the same volume of water (Shimizu, 2008b; Asakawa et al., 2009). Thus, 100 g of organic nanotubes can be readily produced in a laboratory and 10 kg in a factory. As a result, the stable supply of organic nanotubes has become possible, and the searches for applications in many fields have begun in earnest.

This is the first report to examine potential drug delivery application of the organic nanotubes with a carboxyl group (ONTs) at the surface. In this study, the anticancer drug doxorubicin (DXR) was selected for loading into ONTs. DXR has a weak amine group and has been reported to be entrapped into many particle carriers such as polymer micelles, liposomes, and carbon nanotubes (Yokoyama et al., 1991; Cabanes et al., 1998; Liu et al., 2007). Information on ONT loading with DXR will help to compare these

* Corresponding author. Tel.: +81 3 5498 5048; fax: +81 3 5498 5048.
E-mail address: yoshie@hoshi.ac.jp (Y. Maitani).

0378-5173/$ – see front matter © 2011 Elsevier B.V. All rights reserved.
doi:10.1016/j.ijpharm.2011.04.038

different carriers. Loading of DXR into ONT and the release of DXR from ONT were controlled by varying the pH and ionic strength in the medium. ONT loaded with the drug was taken up by non-phagocytic mouse colon adenocarcinoma 26 cell line (C26) cells, and the drug was released quickly in the cells. Furthermore, ONTs were functionalized by associating with a folate-conjugated lipid non-covalently.

2. Materials and methods

2.1. Materials

ONTs were prepared at the Nanotube Research Center (NTRC), National Institute of Advanced Industrial Science and Technology (AIST) (Tsukuba, Japan). ONT1 and ONT2 are easily formed by the evaporating methanol solutions of compounds **1** and **2**, respectively (Fig. 1) (Kogiso et al., 2010a). Gd^{3+}-complexed ONT1 (Gd-ONT1), which contained 12.6 wt% of gadolinium(III) ions, was also formed from $GdCl_3$ and compound **1** as described previously (Kogiso et al., 2010b). Methoxy-poly(ethyleneglycol)-distearylphosphatidylethanolamine (PEG_{2000}-DSPE, PEG mean molecular weight, 2000) and amino-PEG_{2000}-DSPE were purchased from NOF Corporation (Tokyo, Japan). DXR hydrochloride was purchased from Wako Pure Chemical Industries Ltd. (Osaka, Japan). Folate-PEG_{2000}-DSPE conjugate of folic acid (F-PEG-DSPE) was synthesized from amino-PEG-DSPE as reported previously (Gabizon et al., 1999). RPMI-1640 medium, folate-deficient RPMI-1640 medium, and fetal bovine serum (FBS) were obtained from Invitrogen Corp. (Carlsbad, CA, USA). Other reagents used in this study were of reagent grade.

2.2. Cell culture

Mouse colon adenocarcinoma 26 cell line (C26) and a human nasopharyngeal cancer cell line (KB) were obtained from the Cell Resource Center for Biomedical Research, Tohoku University (Miyagi, Japan). The cells were cultured in RPMI-1640 medium or folate-deficient RPMI-1640 medium containing 10% heat-inactivated FBS and 100 μg/mL kanamycin sulfate in a humidified atmosphere containing 5% CO_2 at 37 °C.

2.3. Preparation of ONTs loaded with DXR

2.3.1. DXR loading into ONTs

To prepare ONTs loaded with DXR (DXR/ONT), ground ONT (~2 mg, a length of approximately 2 μm) and DXR aqueous solutions (1 mg/mL, 100 μL) were mixed, then vortexed for 10 min, and sonicated. Then, 900 μL of deionized and filtered water (water), PBS (pH 7.4), or McIlvaine buffer (pH 4, 6, or 8) was added to the mixture of DXR and ONTs. To measure the entrapment efficiency of DXR into ONTs, the mixing weight ratio of ONTs and DXR and the medium were changed. After mixing, DXR and ONT in the medium were centrifuged (20,400 × *g*, 20 °C, 30 min), the precipitate was washed with water (DXR/ONT), and the DXR concentration in the supernatant was analyzed by HPLC (Barth and Conner, 1977). The HPLC system was composed of an LC-20AT pump (Shimadzu Co.), SIL-20A autoinjector (Shimadzu Co.), RF-10AXL fluorescence detector (Shimadzu Co.), and YMC-PACK Pro C18 RS, 150 mm × 4.6 mm i.d. column (YMC Co. Ltd., Kyoto, Japan). The isocratic mobile phase was 3:7 (v/v) acetonitrile:ammonium formate, adjusted to pH 4.0 with formic acid, running at a flow rate of 1.0 mL/min. Daunorubicin was used as the internal standard (i.s.). Daunorubicin and DXR were detected by excitation and emission wavelengths of 485 and 535 nm, respectively. Then, the loading amount and loading efficiency were calculated using the following equations:

$$\text{Loading amount}\,(\mu g/mg) = \frac{\text{added DXR}\,(\mu g) - \text{remained DXR in supernatant}\,(\mu g)}{\text{ONT amount}\,(\mu g)}$$

$$\text{Loading efficiency}\,(\%) = \frac{\text{added DXR}\,(\mu g) - \text{remained DXR in supernatant}\,(\mu g)}{\text{added DXR}\,(\mu g)} \times 100$$

2.3.2. DXR/folate-modified ONT1

DXR/folate-modified ONT1 (DXR/F-ONT1) was prepared by mixing DXR/ONT1 at a weight ratio of 1:20 with PBS at pH 7.4. then, a 0.25, 0.5, or 2.5 mol% of F-PEG-DSPE solution was added to 2 mg/mL DXR/ONT1 suspended in water, which was then incubated overnight and centrifuged at 20,400 × *g* for 30 min at 20 °C to separate DXR/F-ONT1 and free F-PEG.-DSPE. To confirm folate modification, the DXR/F-ONT1 suspension was irradiated with UV light at 253.7 nm for 1 h. After centrifugation at 20,400 × *g* for 30 min, degraded folate (pterine-6-carboxylic acid) in the supernatant was detected using a fluorescence spectrophotometer (Hitachi High-Tech, Tokyo, Japan) with an excitation wavelength of 350 nm and emission wavelength at 350–600 nm. DXR/PEG-modified ONT1 (DXR/PEG-ONT1) was also prepared by the same method using PEG-DSPE instead of F-PEG-DSPE.

2.4. Drug release from ONT1

The release of DXR from DXR/ONT1 in a dialysis tube was measured using seamless cellulose tube membranes (Viskase Sales Corp., IL, USA) with a molecular weight cutoff of 100,000. The initial concentration of DXR was 100 μg/mL. The sample volume in the dialysis tube was 1 mL and the sink volume was 100 mL of PBS at pH 7.4 or 5.5 with the same ionic strength, adjusted by the addition of sodium chloride or water at 37 °C (Johnston et al., 2006). The DXR concentration was analyzed using HPLC as described in Section 2.3.1. The release of DXR from ONT1 at pH 7.4 or pH 5.5 was corrected by characterizing the release of free DXR as adsorption of DXR using the dialysis membrane.

2.5. Cytotoxicity study

C26 or KB cells were prepared by plating 1×10^4 cells in a 96-well culture Plate 1 day before the experiment. Cells were then incubated with the ONTs, DXR, DXR/ONT1 and DXR/F-ONT1 diluted in RPMI-1640 medium or folate-deficient RPMI-1640 medium containing 10% heat-inactivated FBS for 48 h at 37 °C. Cytotoxicity was determined using a WST-8 assay (Dojindo Laboratories, Kumamoto, Japan). The number of viable cells was then determined by absorbance measured at 450 nm using an automated plate reader (BioRad, Hercules, CA, USA).

2.6. Flow cytometry analysis

ONT1 was labeled with 1,1′-dioctadecyl-3,3,3′,3′-perchlorate (DiI) to evaluate cellular uptake. An ethanolic solution of DiI (0.1 mol% of ONT1) was added to the ONT suspension in PBS (pH 7.4), which was incubated for 3 days and then centrifuged 20,400 × *g* at 20 °C for 30 min (DiI-labeled ONT1). The resulting precipitate was resuspended in culture medium. C26 and KB cells were prepared by plating 1×10^6 cells/well in a 6-well culture Plate 1 day before assaying. Cells were incubated with DiI-labeled ONT1 or DXR/F-ONT1 at less than 200 μg/mL ONT1 in RPMI-1640 medium or folate-deficient RPMI-1640 medium, respectively, containing

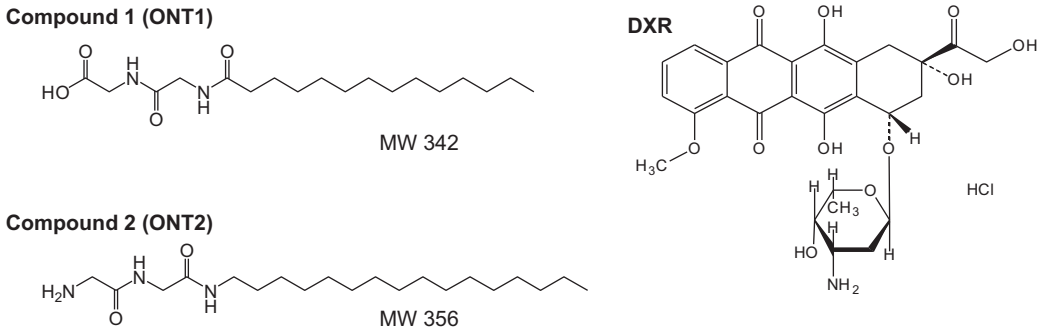

Fig. 1. Chemical structures of compound **1**, compound **2**, and doxorubicin (DXR). Compound **1** forms organic nanotube 1 (ONT1) and compound **2** forms ONT2. Compound **1** consists of glycylglycine and myristic acid, and compound **2** consists of glycylglycine and hexadecylamine.

10% heat-inactivated FBS for 1 or 24 h at 37 °C. After incubation, the cells were washed with cold PBS two times, detached with 0.05% trypsin or EDTA, respectively, and then suspended in PBS containing 0.1% bovine serum albumin and 1 mM EDTA. The suspended cells were directly introduced into a FACSCalibur flow cytometer (Becton Dickinson, San Jose, CA, USA) equipped with a 488 nm argon ion laser. Data for 10,000 fluorescent events were obtained by recording forward scatter and side scatter with 530/30 nm fluorescence. The autofluorescence of cells was taken as a control.

2.7. Confocal microscopy

After incubation with DiI-labeled ONT1 for 1 or 24 h as described above, the medium was removed, and the cells were washed three times with PBS and fixed with 10% formaldehyde in PBS at 37 °C for 20 min. Then, the cells were coated with Aqua Poly/Mount (Polyscience, Warrington, PA, USA) to prevent fading and covered with coverslips. The fixed cells were observed using a LSM5 EXCITER confocal laser scanning microscope (Carl Zeiss, Thornwood, NY, USA). For DiI, maximal excitation was performed using a 543-nm internal He-Neon laser, and fluorescence emission at 565 nm was observed with a LP560. Nucleic acids were stained using SYTOX Green (Invitrogen Corp. Carlsbad, CA, USA), and images were obtained using excitation with an argon laser at 488 nm and fluorescence emission at 523 nm with a filter, BP505-530.

2.8. Determination of cellar uptake of a Gd-ONT1

C26 cells were prepared as a confluent layer in a 10-cm diameter culture plate for the assay. Cells were incubated with 200 μg/mL of Gd-ONT1 in 5 mL of RPMI-1640 medium containing 10% heat-inactivated FBS for 3 h at 37 °C. After incubation, the cells were washed two times with PBS at pH 7.4 and lysed with 1 mL of PBS containing 0.2% Triton X-100 per dish. Associated amounts of Gd in the lysed cells were measured using an inductively coupled plasma (ICP) assay using an SPS7800 apparatus (SII NanoTechnology Inc., Tokyo, Japan). The amount of cellular uptake was calculated using the following equation:

$$\text{Dose}\,(\%) = \frac{\text{cellular uptake of Gd-ONT1}\,(\text{mg})}{\text{applied Gd-ONT1}\,(\text{mg})} \times 100$$

2.9. TEM observation

C26 or KB cells were prepared at 70% confluency on Aclar film (NISSIN EM, Tokyo) 1 day before the experiment. Cells were then incubated with 10 μg/mL ONT1 or F-ONT1 diluted in RPMI-1640 medium or folate-deficient RPMI-1640 medium, respectively containing 10% heat-inactivated FBS for 1 and 24 h at 37 °C. After incubation, the cells were washed three times with PBS at pH 7.4 and fixed with 2% glutaraldehyde in PBS (pH 7.4) for 2 h at 4 °C. After washing, the cells were postfixed with 1% osmium tetroxide in PBS (pH 7.4) for 2 h at 4 °C, and washed again with the same buffer. The fixed specimens were stained with 1% uranyl acetate for 1 h at 4 °C, dehydrated with a graded ethanol series, and embedded in the Quetol 812 mixture (NISSIN EM, Tokyo). Ultrathin sections were stained with 4% uranyl acetate and 0.4% lead citrate and observed using a JEM-1200EXS (JEOL Ltd., Tokyo) at 80 kV.

2.10. Statistical analysis

The results are expressed as the mean ± S.D. Statistical comparisons were performed using Student's *t*-test. *P* values less than 0.05 were considered significant.

3. Results

3.1. Characterization of ONTs

ONT1 had an inner diameter of 30–40 nm, an outer diameter of 70–90 nm, and a gel-to-liquid crystalline phase transition temperature of approximately 60 °C. ONT2 had similar characteristics to ONT1. The cytotoxicity of ONT1 in C26 cells and KB cells was examined. For both cell lines, death was induced at a concentration above 200 μg/mL for ONT1, as shown in Fig. 2. The IC_{50} values for KB cells and C26 cells were 200 and 171.1 μg/mL, respectively. These values are higher than that for conventional liposomes (Kajiwara et al., 2007), suggesting that ONT1 is safe to use.

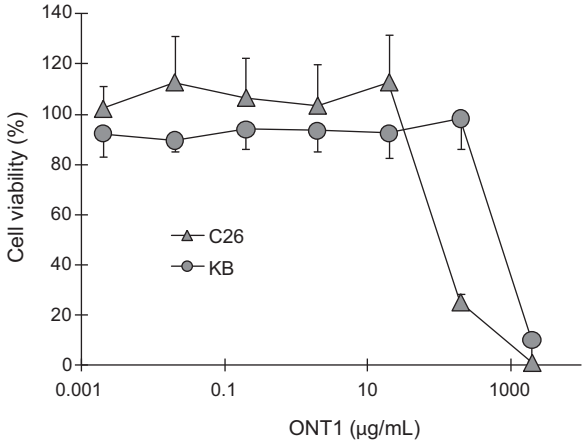

Fig. 2. Cytotoxicity of ONT1 in C26 cells or KB cells treated for 48 h. Each value represents mean ± S.D. ($n = 4$).

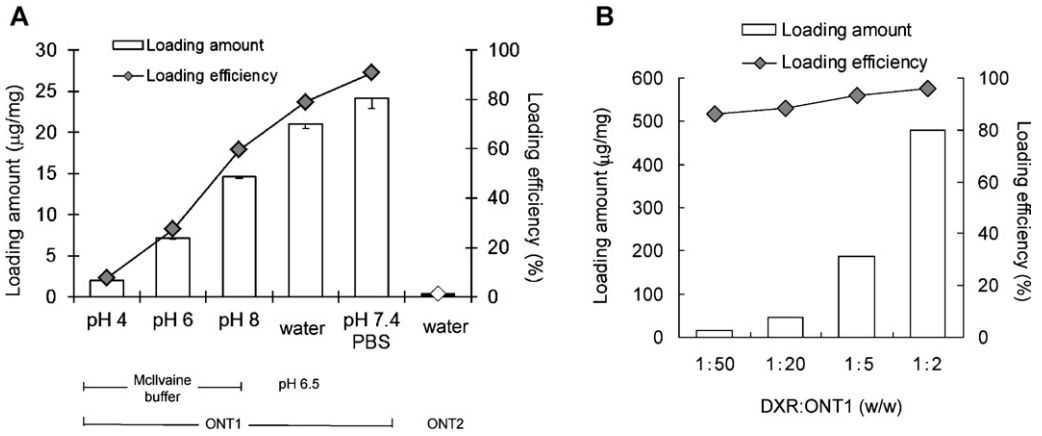

Fig. 3. Loading amount and loading efficiency of DXR into ONTs at a DXR/ONT weight ratio of ~0.05 in various buffers (A) and various ratios of DXR:ONT1 (w/w) in PBS at pH 7.4 (B). Each value represents mean ± S.D. ($n = 3$).

3.2. DXR loading and release from ONT1

First, to examine the effect of pH on the loading of DXR into ONTs, McIlvaine buffer at pH 4, 6, or 8 (ionic strength, 1.0) was used as a medium. DXR loading efficiency into ONT1 at a weight ratio of DXR/ONT of 1:20 increased from 2 to 15 μg DXR/mgONT1 when the pH of the medium was increased from pH 4 to 8 (Fig. 3A). The preparation of DXR/ONT1 using McIlvaine buffer indicated that DXR loading efficiency increased depending on the increasing pH of the medium. Next, to examine the effect of ionic strength on loading efficiency; water and pH 7.4 physiological buffer (PBS, ionic strength, 0.2) were used as the media. Loading efficiency with water at pH 6.5 was substantially higher than that with McIlvaine buffer at the corresponding pH. The loading efficiency with PBS at pH 7.4 was the highest (90%) among those media tested (Fig. 3A). This finding indicated that lower ionic strength and higher pH increased DXR loading. To examine the interaction of the carboxyl group of ONT1 with DXR, ONT2 with an amino group was used. In contrast, DXR in water was hardly loaded into ONT2.

Next, the effect of the weight ratio of DXR and ONT1 on DXR loading was examined (Fig. 3B). As the DXR:ONT1 ratio increased, DXR loading increased to 480 μg/mg. A weight ratio of DXR:ONT1 = 1:20 in PBS at pH 7.4 was selected as the drug loading condition in the following experiment because of the adequate loading efficiency (88%), the amount loaded (44.2 μg/mg), and the easy of handling. The DXR/ONT1 was confirmed to retain nanotube structure using microscope because non-spherical size was not able to measure using dynamic light scattering method.

DXR release from the DXR/ONT1 prepared as described above was evaluated for 72 h in water or PBS at pH 7.4 and 5.5. DXR was not released from DXR/ONT1 in water (data not shown). The release of DXR from ONT1 in PBS at pH 5.5 was promoted compared with that at pH 7.4 (Fig. 4).

3.3. Cellular uptake of ONT1

To evaluate the cellular uptake of ONT1 itself, DiI-labeled ONT1 was incubated with C26 cells for 1 and 24 h. Intracellular fluorescence of DiI-labeled ONT1 increased significantly in a time-dependent manner, as detected by flow cytometry (Fig. 5A). In addition, the cellular uptake of DXR/ONT1 was evaluated by cytotoxicity at a concentration of ONT1 below its IC_{50}. DXR/ONT1 exhibited cell death and apoptosis using a 48 h incubation period, similar to free DXR (Fig. 5B). The IC_{50} between DXR and DXR/ONT1 was not significantly different. Separately, it was confirmed that drug release from DXR/ONT1 in the culture medium was less than 20% (date not shown).

C26 cells incubated with DiI-labeled ONT1, as shown in Fig. 5A, were also observed using confocal microscopy. Red fluorescence of DiI-labeled ONT1 in the cytoplasm was observed with an increasing incubation time for 1–24 h (Fig. 6A and B). Furthermore, it revealed that ONT1 had very high affinity to the cells because a lot of ONT1 was observed on the cellular surface when incubated for 24 h (Fig. 6C).

Because there is the possibility that DXR released from ONT1 could penetrated into cells, the cellular uptake of Gd-ONT1 was examined. Unlike DXR, conjugated Gd was not released from Gd-ONT1, and free Gd ions cannot penetrate into the cells. Gd concentration in the cell lysis fraction after a 3-h incubation of the Gd-ONT1 with C26 cells was determined. The 0.05% dose of Gd was detected in the cells. Moreover, it was confirmed by TEM that ONT1 and F-ONT1 were present in C26 cells (Fig. 7) and KB cells (data not shown), respectively. As shown in Fig. 7B and C, ONT1 was observed in the cytoplasm near the cell membrane after a 24-h incubation, compared with control, untreated C26 cells (Fig. 7A). From these, the finding indicated that ONT1 was taken up to the cells.

3.4. ONT1 functionalized with folate

3.4.1. Confirmation of folate modification

To functionalize ONT1 for cellular uptake mediated by folate receptors (FR), folate-modified ONT1 loaded with DXR (DXR/F-ONT1) and PEGylated ONT1 loaded with DXR (DXR/PEG-

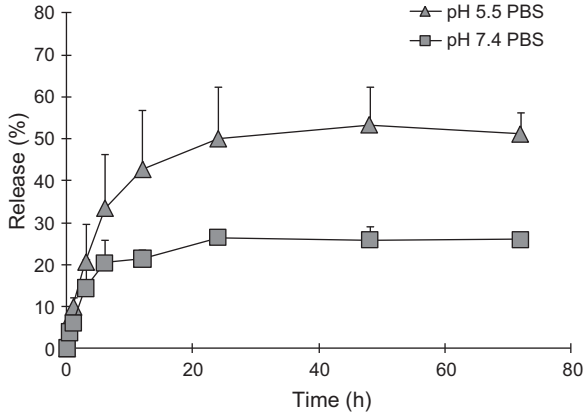

Fig. 4. DXR release from DXR/ONT1 in PBS at pH 5.5 and pH 7.4. Each value represents mean ± S.D. ($n = 3$).

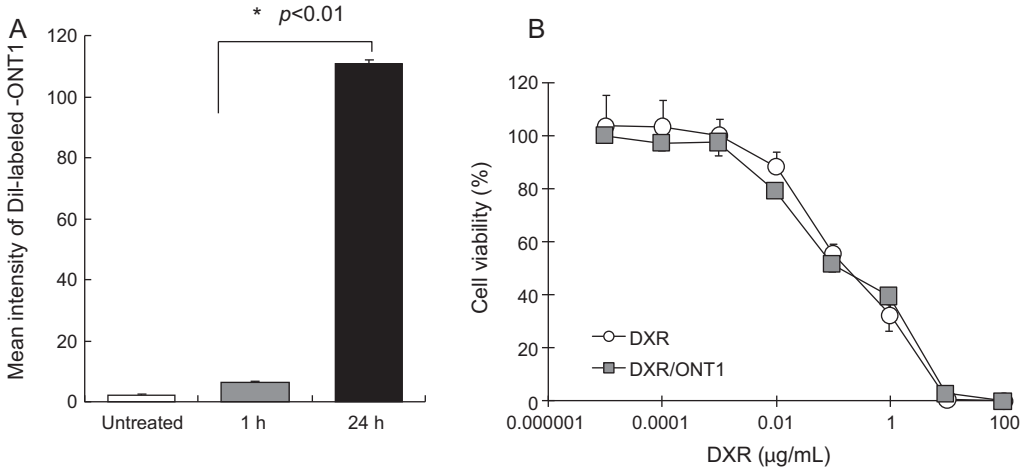

Fig. 5. Evaluation of cellular uptake of ONT1. Cellular uptake of DiI-labeled ONT1 into C26 cells incubated for 1 or 24 h assessed by flow cytometry analysis ($n = 3$) (A). Cytotoxicity of free DXR and DXR/ONT1 in C26 cells incubated for 48 h ($n = 4$) (B). Each value represents mean ± S.D.

ONT1) as a control were prepared. The folate modification was confirmed using fluorescence detection of pterine-6-carboxylic acid, which is a degradation product of folate after UV irradiation (Akhtar et al., 1999; Hirakawa et al., 2003). As a result of UV irradiation, the fluorescence intensity of DXR/F-ONT1 at 273.5 nm increased depending on the folate modification of ONT1 while no fluorescence of DXR/PEG-ONT1 was detected (Fig. S1). This finding indicated that ONT1 was modified by folate, depending on addition amount of F-PEG-DSPE.

3.4.2. Cellular uptake of F-ONT1

The cellular uptake of DXR/F-ONT1 was investigated by incubation with FR overexpressed in KB cells. DXR/F-ONT1 was modified with various F-PEG-DSPE concentrations (0.25, 0.5, or 2.5 mol% of ONT1), and cellular uptake of DXR/F-ONT1 was evaluated by flow cytometry after 3 h exposure to KB cells. Using a competition assay with free folic acid, the cellular fluorescence intensity of DXR/F-ONT1 modified with 0.5 or 2.5 mol% folate decreased significantly whereas that of DXR/PEG-ONT1 modified with 2.5 mol% PEG-DSPE was not (Fig. 8A). To assess the cellular uptake, the cytotoxicity of DXR/ONT1 modified with 0.25 mol% folate to KB cells was evaluated. The IC_{50} values of DXR/F-ONT1 (0.074 μM) were similar to that of DXR/ONT1 (0.043 μM) and slightly higher than that of free DXR (0.028 μM) (Fig. 8B). This finding suggested that cellular uptake of DXR/F-ONT1 and DXR/ONT1 was similarly fast.

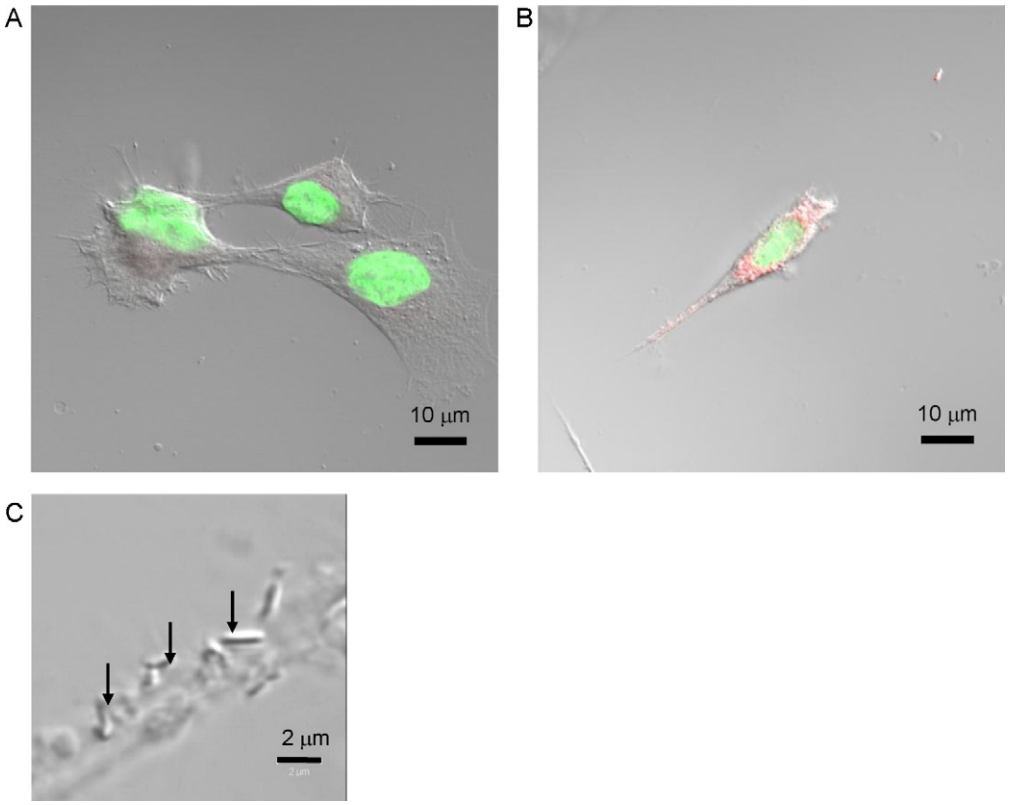

Fig. 6. Cellular uptake of DiI-labeled ONT1 into C26 cells incubated for 1 h (A) or 24 h (B). Red fluorescence indicates DiI and green is a nucleus stained by SYTOX Green. Many ONT1s (arrowhead) were observed at the surface of C26 cells incubated with DiI-labeled ONT1 for 24 h (C).

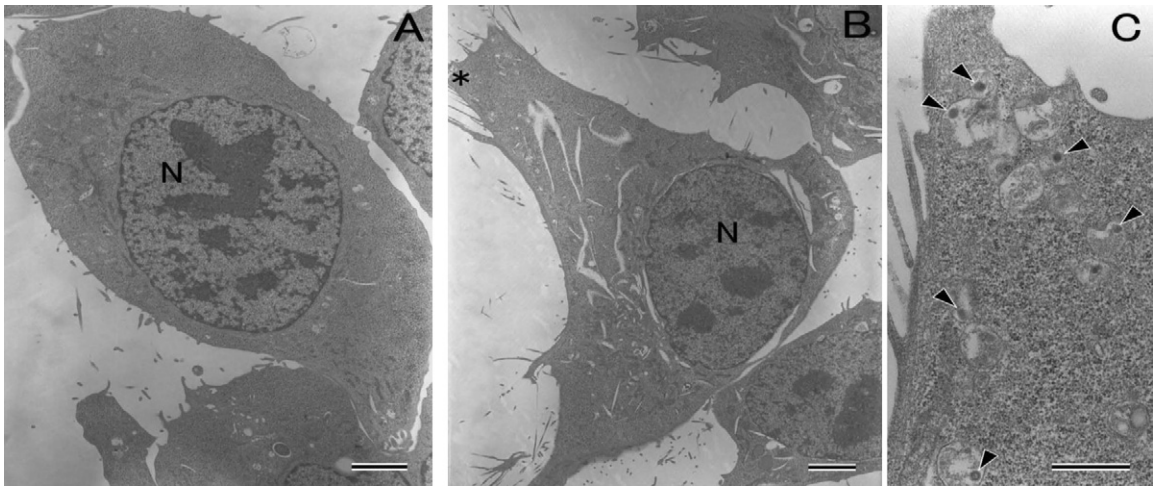

Fig. 7. Transmission electron micrographs showing untreated C26 cells (A) and C26 cells incubated with ONT1 for 24 h (B) and a high magnification image of the surrounding cell (indicated by an asterisk in B) (C). N: nucleus; arrowhead: ONT1, bars = 2 μm (A and B) and 500 nm (C).

4. Discussion

This study showed that at higher pH and a lower ionic strength of the medium, high loading efficiency of DXR into ONT1 and low release of DXR from ONT1 were obtained where the carboxyl group of ONT1 was highly dissociated. Cellular uptake of the DiI-labeled ONT1 into C26 cells was observed by flow cytometry analysis and confocal microscopy. It was also confirmed that Gd-ONT1was detected in the cells and many ONT1s were observed in the endosomes by TEM.

In order to apply ONTs as a drug carrier, their cytotoxicity is of key importance. The cytotoxicity of ONTs in C26 cells and KB cells (IC_{50} 200 and 171.1 μg/mL, respectively) was very low compared with a conventional liposome IC_{50} (8.6 μg/mL) (Kajiwara et al., 2007). Furthermore, it is expected that ONT1 is biodegradable because it is made from edible materials. Thus, ONTs have suitable properties for use as drug carriers.

Drug loading ability and cellular uptake of ONTs were examined using DXR as a model drug because it exhibits autofluorescence and apoptosis inducing activity. ONTs have a nanoscale cylindrical structure; therefore, DXR/ONT was prepared by simply mixing ONT powder with DXR solution by capillary phenomenon. When DXR/ONT was prepared in McIlvaine buffer, the amount of DXR loaded was pH dependent. Higher drug loading efficiency was obtained in PBS at pH 7.4 and lower ionic strength. This result indicated that drug loading into ONT1 was susceptible to the effect of ionic strength and H^+ concentration. The functional group is exposed on the ONT surface, which was supported both by FT-IR spectrum of ONT and by the adsorption of surface-modified gold nanoparticles onto ONT (Kogiso et al., 2010a). ONT1 with a carboxyl group and ONT2 with amino group on their surfaces induced higher and lower levels of DXR loading, respectively. It was supposed that the carboxyl group of ONT1 may interact electrostatically with the amino group of DXR at higher pH where the carboxyl group of ONT1 was highly dissociated. This interaction was decreased in a medium containing electrolytes by electric shielding; therefore, a lower ionic strength of the medium is favorable for preparation of DXR/ONT1.

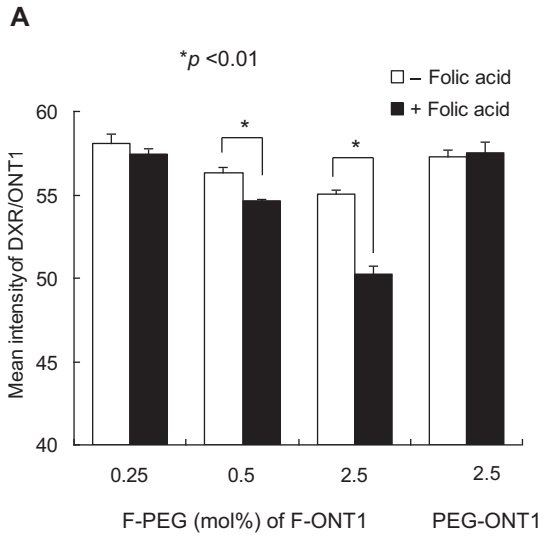

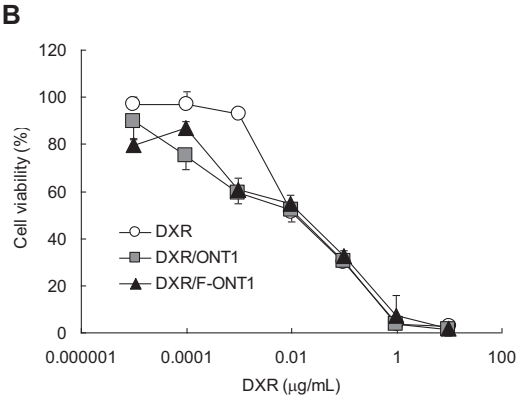

	IC_{50} (μM)
DXR	0.028
DXR/ONT1	0.043
DXR/F-ONT1	0.074

Fig. 8. Evaluation of cellular uptake of ONT1 modified with folate. Cellular uptake of DXR/F-ONT1 and DXR/PEG-ONT1 into KB cells incubated for 3 h was assessed by flow cytometry analysis ($n = 3$) (A). Cytotoxicity of free DXR, DXR/ONT1, and DXR/F-ONT1 modified with 0.25 mol% folate in KB cells incubated for 48 h ($n = 4$) (B). Each value represents mean ± S.D.

The number of carboxylic group per ONT1 is about 2,760,000 estimated using an inner diameter of 50 nm, outer diameter of 80 nm, and length of 2 μm. If the carboxylic group of ONT1 interacts in a 1:1 ratio with an amino group of DXR, 274 μg of DXR will be loaded theoretically into 1 mg of ONT1. In this study, the maximum amount of drug loading was 480 μg DXR/mg ONT1 in a preparation with a 1:2 weight ratio of DXR to ONT1. The DXR loading value was higher compared with that of liposomes (Gokhale et al., 1996). This finding suggested that DXR may insert into each layer.

The release of DXR from ONT1 in PBS at lower pH was higher than that in water. This may be due to a reduction in the electrostatic interaction between DXR and ONT1 because dissociation of the carboxyl group of ONT1 at lower pH and in the presence of electrolytes was reduced. Endosomes are known to function with a typical internal pH value of 5.5 (Wattiaux et al., 2000; Medina-Kauwe et al., 2005), and it was suggested that when DXR/ONT1 was taken up via the endocytotic pathway, the drug should be released quickly from the endosome and will be able to exert its activity. Therefore, drug release from ONT1 at lower pH could be exploited for drug delivery applications for tumor targeting.

Cellular uptake of ONT was evaluated as the cytotoxicity of the loaded DXR activity, which induces apoptosis by intercalation to DNA. The cytotoxic effect of DXR/ONT1 in C26 cells was similar to free DXR. Cellular uptake of DXR/ONT1 and intracellular drug release may occur as rapidly as for free DXR, and/or ONT1 might promote DXR uptake via a specific interaction with the cells. Flow cytometry analysis and confocal microscopy showed time-dependent cellular uptake of the DiI-labeled ONT1 into C26 cells. Gd was detected at a 0.05 dose % in C26 cells incubated with Gd-ONT1 for 24 h. In addition, many ONT1 s were observed in the endosomes by TEM. Although the cellular uptake mechanisms of ONT1 are not clear at present, these results suggest that ONT1 may have high affinity for these cells, and may play an important role in the cellular uptake of the ONT1.

To provide a further possibility for use as a drug carrier, the active targeting ability of ONT1 modified with a target ligand was evaluated. In this study, we focused on cellular uptake via FR. It is known that FR is overexpressed in many human cancer cells, including malignancies of the ovary, mammary gland, kidney, lung, and throat, but is expressed minimally in normal tissues (Kelemen, 2006). Therefore, FR is a good target for selective cancer therapy as a tumor-specific receptor. FRα has a high affinity for folic acid (Kd ~ 0.1 nM; Kamen and Caston, 1986), and its conjugate retains its receptor binding and endocytosis properties in FR positive cancer cells (Leamon and Low, 1991; Anderson et al., 1992; Lu and Low, 2002). We prepared DXR/folate-modified ONT1, DXR/F-ONT1, and evaluated its cellular uptake via FR in KB cells. The cytotoxicity of DXR/F-ONT1 was not significantly different with that of DXR/ONT1. Corresponding to an increase of the modification amount of folate, a competition assay demonstrated that the cellular uptake of DXR/F-ONT1 decreased although the total uptake amount did not increase. It was supposed that cellular pathway through FR for DXR/F-ONT1 uptake and other pathways such as specific for ONT may exist. Therefore, with the addition of free folic acid, increased cellular uptake via FR was not detected, and only inhibition of FR-mediated endocytosis was observed. ONT1 is expected to be an excellent active targeting carrier if folate modification of ONT makes it possible to increase cellular uptake via FR above that for ONT-specific uptake.

5. Conclusions

In this study, we examined the potential of ONT as a drug carrier and demonstrated the following findings; ONT1 can load 480 μg DXR/mg ONT and release the drug rapidly in an acidic environment. DXR/ONT1 was taken up by cells and the drug was released quickly into the cells. Moreover, ONT1 was able to be modified by simply mixing with a folate lipid, which was then taken up through FR. Therefore, these novel, biodegradable organic nanotubes have the potential to be used as drug carriers for controlled and targeted drug delivery. This is the first report on the application of ONTs as drug carriers; however, further in vitro evaluation of interactions with cells must be investigated before this approach can be applied in vivo.

Acknowledgement

This study was supported in part by the Open Research Center Project.

Appendix A. Supplementary data

Supplementary data associated with this article can be found, in the online version, at doi:10.1016/j.ijpharm.2011.04.038.

References

Akhtar, M.J., Khan, M.A., Ahmad, I., 1999. Photodegradation of folic acid in aqueous solution. J. Pharm. Biomed. Anal. 19, 269–275.
Anderson, R.G., Kamen, B.A., Rothberg, K.G., Lacey, S.W., 1992. Potocytosis: sequestration and transport of small molecules by caveolae. Science 255, 410–411.
Asakawa, M., Aoyagi, M., Kameta, N., Kogiso, M., Masuda, M., Minamikawa, H., Shimizu, T., 2009. Development of massive synthesis method of organic nanotube toward practical use. Synthesiology – English Ed. 1, 169–176.
Bangham, A.D., Standish, M.M., Watkins, J.C., 1965. Diffusion of univalent ions across the lamellae of swollen phospholipids. J. Mol. Biol. 13, 238–252.
Barth, H.G., Conner, A.Z., 1977. Determination of doxorubicin hydrochloride in pharmaceutical preparations using high-pressure liquid chromatography. J. Chromatogr. 131, 375–381.
Cabanes, A., Tzemach, D., Goren, D., Horowitz, A.T., Gabizon, A., 1998. Comparative study of the antitumor activity of free doxorubicin and polyethylene glycol-coated liposomal doxorubicin in a mouse lymphoma model. Clin. Cancer Res. 4, 499–505.
Gabizon, A., Horowitz, A.T., Goren, D., Tzemach, D., Mandelbaum-Shavit, F., Qazen, M.M., Zalipsky, S., 1999. Targeting folate receptor with folate linked to extremities of poly(ethylene glycol)-grafted liposomes: in vitro studies. Bioconjug. Chem. 10, 289–298.
Gokhale, P.C., Radhakrishnan, B., Husain, S.R., Abernethy, D.R., Sacher, R., Dritschilo, A., Rahman, A., 1996. An improved method of encapsulation of doxorubicin in liposomes: pharmacological, toxicological and therapeutic evaluation. Br. J. Cancer 74, 43–48.
Gratton, S.E., Ropp, P.A., Pohlhaus, P.D., Luft, J.C., Madden, V.J., Napier, M.E., DeSimone, J.M., 2008. The effect of particle design on cellular internalization pathways. Proc. Natl. Acad. Sci. U.S.A. 105, 11613–11618.
Hirakawa, K., Suzuki, H., Oikawa, S., Kawanishi, S., 2003. Sequence-specific DNA damage induced by ultraviolet A-irradiated folic acid via its photolysis product. Arch. Biochem. Biophys. 410, 261–268.
John, G., Masuda, M., Okada, Y., Yase, K., Shimizu, T., 2001. Nanotube formation from renewable resources via coiled nanofibers. Adv. Mater. 13, 715–718.
Johnston, M.J., Semple, S.C., Klimuk, S.K., Edwards, K., Eisenhardt, M.L., Leng, E.C., Karlsson, G., Yanko, D., Cullis, P.R., 2006. Therapeutically optimized rates of drug release can be achieved by varying the drug-to-lipid ratio in liposomal vincristine formulations. Biochim. Biophys. Acta 1758, 55–64.
Kajiwara, E., Kawano, K., Hattori, Y., Fukushima, M., Hayashi, K., Maitani, Y., 2007. Long-circulating liposome-encapsulated ganciclovir enhances the efficacy of HSV-TK suicide gene therapy. J. Control. Release 120, 104–110.
Kamen, B.A., Caston, J.D., 1986. Properties of a folate binding protein (FBP) isolated from porcine kidney. Biochem. Pharmacol. 35, 2323–2329.
Kameta, N., Masuda, M., Shimizu, T., 2005. Selective construction of supramolecular nanotube hosts with cationic inner surfaces. Adv. Mater. 17, 2732–2736.
Kameta, N., Masuda, M., Minamikawa, H., Mishima, Y., Yamashita, I., Shimizu, T., 2007. Functionalizable organic nanochannels based on lipid nanotubes; encapsulation and nanofluidic behavior of biomacromolecules. Chem. Mater. 19, 3553–3560.
Kameta, N., Minamikawa, H., Masuda, M., Mizuno, G., Shimizu, T., 2008. Controllable biomolecule release from self-assembled organic nanotubes with asymmetric surfaces: pH and temperature dependence. Soft Matter 4, 1681–1687.
Kamiya, S., Minamikawa, H., Jung, J.H., Yang, B., Masuda, M., Shimizu, T., 2005. Molecular structure of glucopyranosylamide lipid and nanotube morphology. Langmuir 21, 743–750.
Kelemen, L.E., 2006. The role of folate receptor alpha in cancer development, progression and treatment: cause, consequence or innocent bystander? Int. J. Cancer 119, 243–250.

Kogiso, M., Zhou, Y., Shimizu, T., 2007. Instant preparation of self-assembled metal-complexed lipid nanotubes that act as self-templates to produce metal-oxide nanotubes. Adv. Mater. 19, 242–246.
Kogiso, M., Aoyagi, M., Asakawa, M., Shimizu, T., 2010a. Highly efficient production of organic nanotubes with various surfaces and their application as adsorbents. Soft Matter 6, 4528–4535.
Kogiso, M., Aoyagi, M., Asakawa, M., Shimizu, T., 2010b. Semi-solid phase synthesis of metal-complexed organic nanotubes. Chem. Lett. 39, 822–823.
Leamon, C.P., Low, P.S., 1991. Delivery of macromolecules into living cells: a method that exploits folate receptor endocytosis. Proc. Natl. Acad. Sci. U.S.A. 88, 5572–5576.
Liu, Z., Sun, X., Nakayama-Ratchford, N., Dai, H., 2007. Supramolecular chemistry on water-soluble carbon nanotubes for drug loading and delivery. ACS Nano 1, 50–56.
Lu, Y., Low, P.S., 2002. Folate-mediated delivery of macromolecular anticancer therapeutic agents. Adv. Drug Deliv. Rev. 54, 675–693.
Medina-Kauwe, L.K., Xie, J., Hamm-Alvarez, S., 2005. Intracellular trafficking of non-viral vectors. Gene Ther. 12, 1734–1751.
Nakashima, N., Asakuma, S., Kim, J., Kunitake, T., 1984. Helical superstructures are formed from chiral ammonium bilayers. Chem. Lett. 10, 1709–1712.
Shimizu, T., Masuda, M., Minamikawa, H., 2005. Supramolecular nanotube architectures based on amphiphilic molecules. Chem. Rev. 105, 1401–1443.
Shimizu, T., 2006. Self-assembled lipid nanotube hosts: the dimension control for encapsulation of nanometer-scale guest substances. J. Polym. Sci. Part A: Polym. Chem. 44, 5137–5152.
Shimizu, T., 2008a. Self-assembled organic nanotubes: toward attoliter chemistry. J. Polym. Sci. Part A: Polym. Chem. 46, 2601–2611.
Shimizu, T., 2008b. Molecular self-assembly into one-dimensional nanotube architectures and exploitation of their functions. Bull. Chem. Soc. Jpn. 81, 1554–1566.
Wattiaux, R., Laurent, N., Wattiaux-De, C.S., Jadot, M., 2000. Endosomes, lysosomes: their implication in gene transfer. Adv. Drug Deliv. Rev. 41, 201–208.
Yager, P., Schoen, P.E., 1983. Formation of tubules by a polymerizable surfactant. Mol. Cryst. Liq. Cryst. 106, 371–381.
Yamada, K., Ihara, H., Ide, T., Fukumiti, T., Hirayama, C., 1984. Formation of helical super structure from single-walled bilayers by amphiphiles with oligo-L-glutamic acid-head group. Chem. Lett. 10, 1713–1716.
Yang, B., Kamiya, S., Yoshida, K., Shimizu, T., 2004a. Confined organization of Au nanocrystals in glycolipid nanotube hollow cylinders. Chem. Commun. 2004, 500–501.
Yang, B., Kamiya, S., Shimizu, Y., Koshizaki, N., Shimizu, T., 2004b. Glycolipid nanotube hollow cylinders as substrates: fabrication of one-dimensional metallic-organic nanocomposites and metal nanowires. Chem. Mater. 16, 2826–2831.
Yokoyama, M., Okano, T., Akurai, Y., Kimoto, H., Hibazaki, C., Kataoka, K., 1991. Toxicity and antitumor activity against solid tumors of micelle-forming polymeric anticancer drug and its extremely long circulation in blood. Cancer Res. 51, 3229–3236.
Yui, H., Shimizu, Y., Kamiya, S., Masuda, M., Yamashita, I., Ito, K., Shimizu, T., 2005. Encapsulation of ferritin within a hollow cylinder of glycolipid nanotubes. Chem. Lett. 34, 232–233.